Synthesis, Characterization, and Thermal Behavior of Polydentate Ligand Adducts of Barium Trifluoroacetate

William A. Wojtczak, Mark J. Hampden-Smith,* and Eileen N. Duesler

Department of Chemistry and Center for Micro-Engineered Materials, University of New Mexico, Albuquerque, New Mexico 87131

Received October 31, 1996

The reaction of BaH_2 with polydentate ligands and CF_3COOH in THF at −40 °C in 1:1:2 stoichiometries leads to compounds of general formula $[Ba(O_2CCF_3)_2]_mL_n$ (L = 12-crown-4 (**1**), triglyme (**2**), 2-(hydroxymethyl)-15-crown-5 (15-crown-5CH_2OH) (**3**), cryptand(222) (**4**), 18-crown-6·C_5H_5N (**5**), 2-(hydroxymethyl)-18-crown-6 (18-crown-6CH_2OH) (**6**)). A sulfonate compound, $Ba(O_3SCF_3)_2$(tetraglyme) (**7**), was also prepared by a similar reaction. The polydentate ligands of **1**−**6** are coordinated to the barium atoms through all of their donating atoms, and the trifluoroacetate ligands are found in four distinct types of bonding modes. The compounds were characterized by spectroscopic and analytical methods, and **1**−**6** are among the first examples of group 2 trifluoroacetate compounds with mononuclear or dinuclear structures in the solid state as determined by single-crystal X-ray diffraction. $Ba_2(O_2CCF_3)_4$(12-crown-4)$_2$ (**1**) crystallizes from ethanol in monoclinic space group $P2_1/n$ with a = 11.014(1) Å, b = 12.016(1) Å, c = 15.269(1) Å, β = 104.47(1)°, and Z = 4. $Ba_2(O_2CCF_3)_4$(triglyme)$_2$ (**2**) crystallizes from ethanol in monoclinic space group $P2_1/n$ with a = 11.203(1) Å, b = 12.220(1) Å, c = 15.451(1) Å, β = 107.61(1)°, and Z = 4. $Ba_2(O_2CCF_3)_4$(15-crown-5CH_2OH)$_2$ (**3**) crystallizes from ethanol in monoclinic space group $P2_1/c$ with a = 12.445(2) Å, b = 12.499(3) Å, c = 15.615(2) Å, β = 111.11 (1)°, and Z = 4. $Ba(O_2CCF_3)_2$(cryptand(222)) (**4**) crystallizes from toluene in the tetragonal space group $P4_32_12$ with $a = b$ = 9.263(2) Å, c = 35.897(7) Å, and Z = 4. $Ba(O_2CCF_3)_2$(18-crown-6)(py) (**5**) crystallizes from pyridine in orthorhombic space group *Pnma* with a = 27.178(3) Å, b = 11.417(1) Å, c = 9.133(1) Å, and Z = 4. $Ba(O_2CCF_3)_2$(18-crown-6CH_2OH) (**6**) crystallizes from ethanol in monoclinic space group *Pn* with a = 8.279(1) Å, b = 11.410(1) Å, c = 13.661(2) Å, β = 98.41(1)°, and Z = 2. Infrared spectroscopy on **1**−**6** supplied information on the relationships among $\nu_{asym}(CO_2)$, bonding mode of the trifluoroacetate ligand, and donating ability of the polydentate ligand. Thermogravimetric analysis of **1**−**7** shows loss of the organic supporting ligands in the temperature range 250−600 °C with formation of BaF_2.

Introduction

There has been a great deal of recent interest in the synthesis of compounds which can be used as precursors for the formation of films containing the group 2 elements, particularly Ca, Sr, and Ba. Films are formed primarily from the liquid phase (e.g. spin coating or dip coating) or from the gas phase (e.g. by chemical vapor deposition, CVD).[1−3] In the case of the group 2 compounds, the synthesis of precursors with properties suitable for CVD (volatility and reactivity)[4] is extremely challenging because of the large size of the lower group 2 elements and the resulting tendency for oligomerization and, therefore, a decrease in volatility. Group 2 species that have been primarily studied as precursors to group 2 element-containing films are the β-diketonate derivatives.[2,5−11] These derivatives contain the most volatile group 2 species discovered to date and have lead to the successful deposition of group 2 containing films, such as MF_2[12] and $MTiO_3$.[13−19] However, in the case of deposition of metal titanate and other metal oxide films, water[6,14−16,18,20−22] is often added as a reagent in an attempt to remove cleanly the β-diketonate ligand by hydrolysis, according to the equation of reaction 1.

However, water also reacts with other reagents in the system, such as metal alkoxides, and can cause hydrolysis which may lead to detrimental side reactions, such as particle formation.

* To whom correspondence should be addressed.

(1) Wojtczak, W. A.; Fleig, P.; Hampden-Smith, M. J. In *Advances in Organometallic Chemistry*; Academic Press: New York, 1996; Vol. 31.
(2) Marks, T. J. *Pure Appl. Chem.* **1995**, *67*, 313−318.
(3) Barron, A. R.; Rees, W. S. *Adv. Mater. Opt. Elec.* **1993**, *2*, 271−288.
(4) *CVD of Nonmetals*; Rees, W. S., Ed.; VCH: Weinheim, Germany, 1996.
(5) Malandrino, G.; Fragala, I. L.; Neumayer, D. A.; Stern, C. L.; Hinds, B. J.; Marks, T. J. *J. Mater. Chem.* **1994**, *4*, 1061−1066.
(6) Neumayer, D. A.; Studebaker, D. B.; Hinds, B. J.; Stern, C. L.; Marks, T. J. *Chem. Mater.* **1994**, *6*, 878−80.
(7) Schulz, D. L.; Hinds, B. J.; Stern, C. L.; Marks, T. J. *Inorg. Chem.* **1993**, *32*, 249−250.
(8) Schulz, D. L.; Hinds, B. J.; Neumayer, D. A.; Stern, C. L.; Marks, T. J. *Chem. Mater.* **1993**, *5*, 1605−1617.
(9) Timmer, K.; Spee, K. I. M. A.; Mackor, A.; Meinema, H. A.; Spek, A. L.; Van der Sluis, P. *Inorg. Chim. Acta* **1991**, *190*, 109−17.
(10) Van der Sluis, P.; Spek, A. L.; Timmer, K.; Meinema, H. A. *Acta Crystallogr., Sect. C* **1990**, *46*, 1741.
(11) Norman, J. A. T.; Pez, G. P. *J. Chem. Soc., Chem. Commun.* **1991**, *14*, 971−2.
(12) Purdy, A. P.; Berry, A. D.; Holm, R. T.; Fatemi, M.; Gaskill, D. K. *Inorg. Chem.* **1989**, *28*, 2799−803.
(13) Gilbert, S. R.; Wessels, B. W.; Studebaker, D. B.; Marks, T. J. *Appl. Phys. Lett.* **1995**, *66*, 3298−300.
(14) Feil, W. A.; Wessels, B. W.; Tonge, L. M.; Marks, T. J. *J. Appl. Phys.* **1990**, *67*, 3858−61.
(15) Richeson, D. S.; Tonge, L. M.; Zhao, J.; Zhang, J.; Marcy, H. O.; Marks, T. J.; Wessels, B. W.; Kannewurf, C. R. *Appl. Phys. Lett.* **1989**, *54*, 2154−6.
(16) Wills, L. A.; Wessels, B. W.; Richeson, D. S.; Marks, T. J. *Appl. Phys. Lett.* **1992**, *60*, 41−3.

S0020-1669(96)01322-5 CCC: $15.00
Published on Web 04/03/1998

$$\text{Ba}(\beta\text{-diketonate})_2 + 2\text{H}_2\text{O} \rightarrow \text{“Ba(OH)}_2\text{”} + 2\beta\text{-diketone} \quad (1)$$

Therefore it would be desirable to have an alternative reagent to β-diketonates as precursors for delivering the group 2 component in these systems. A number of other ligands have been investigated such as cyclopentadienides[23−25] and Schiff bases[7,8] with fairly limited success. Our approach has been to investigate whether carboxylate derivatives with suitable volatility can be prepared and, if so, whether they undergo ester-elimination reactions with metal alkoxides[26,27] to form mixed-metal oxides. This was recently demonstrated for a number of Group 14 carboxylates according to eq 2.

$$\text{M}(\text{O}_2\text{CR})_n + \text{M}'(\text{OR}')_n \rightarrow [\text{MM}'(\text{O})_{n-m/2}(\text{O}_2\text{CR})_{n-m}(\text{OR})_{n-m}] + (n-m)\text{RCO}_2\text{R}' \quad (2)$$

This reaction has potential because it results in elimination of the organic supporting ligands, thereby avoiding contamination, and results in formation of oxo bridges between the metals which are desired in the final crystalline film. The potential for the reaction between group 2 metal carboxylates and metal alkoxides to form $BaTiO_3$, $SrTiO_3$, and $Ba_{1-x}Sr_xTiO_3$ films by liquid phase routes was recently demonstrated.[28] It should be noted that metal carboxylates and metal oxalates have been used extensively as precursors to inorganic materials.[29,30]

There are very few examples of carboxylate derivatives of group 2 elements that are likely to be suitable for CVD. Most derivatives are oligomeric. There are a few examples of monomeric species such as $Ba(O_2CCH_3)_2$(18-crown-6)·$4H_2O$[31] and Ba(pivalate)$_2$(18-crown-6),[32] but they either possess coordinated water, which would be detrimental to both the volatility of the species and also reaction with metal alkoxides, or they lose their polydentate ligand prior to being vaporized. Here, we report the results of a study of the synthesis and characterization of a number of barium carboxylate derivatives with polydentate donor ligands. The fluorinated carboxylate, trifluoroacetate, was chosen because it was expected that the presence of fluorinated ligands might enhance volatility, and polydentate ligands were used to reduce the degree of oligomerization as has been demonstrated in the analogous β-diketonate derivatives. The focus of this study is to understand the structural variety in these compounds, determine the diversity of carboxylate ligand coordination modes possible, and explore the thermal and transport properties of these compounds.

Experimental Section

All reactions were carried out under a nitrogen atmosphere by using standard vacuum-line and Schlenk techniques. The solvents were predried over molecular sieves and distilled under nitrogen from the appropriate drying reagents. BaH_2, 12-crown-4, triglyme, 18-crown-6, tetraglyme, 2-hydroxy-18-crown-6 (18-crown-6CH_2OH), 2-hydroxy-15-crown-5 (15-crown-5CH_2OH), cryptand(222) (4,7,13,16,21,24-hexaoxa-1,10-bicyclo[8...8...8]hexacosane), CF_3COOH, and CF_3SO_3H were purchased from Aldrich and used as received. ^{1}H and ^{13}C NMR spectra were collected on Bruker AC-250 spectrometers. The IR spectra were obtained as KBr pellets using crystalline materials on a Perkin-Elmer 1600 FTIR spectrophotometer. The IR spectra of **1**−**7** obtained in this way were compared to spectra obtained using the Nujol mull method and found to be substantially the same, indicating that no pressure-induced changes in the spectra occurred by the KBr method (such as anion exchange). The thermogravimetric analyses were conducted in air on a Perkin-Elmer TGA-7 analyzer, and the residues were analyzed by powder X-ray diffraction on a Siemens D5000 diffractometer. Elemental analysis was performed at the University of New Mexico.

In a typical preparation, BaH_2 (1.393 g, 10 mmol) was transferred to a round-bottom flask in a glovebox. The flask was connected to a Schlenk line, and 50 mL of THF was added by cannula with rapid stirring. 12-crown-4 (1.62 mL, 10 mmol) was then added dropwise, followed by cooling to −40 °C and addition of CF_3COOH (1.54 mL, 20 mmol). On slow warming to room temperature, the reaction solution rapidly effervesced and a white precipitate formed. The solution was stirred for 3 h, and then the THF was removed in vacuo. The white precipitate was dissolved in a minimum amount of dry ethanol (ca. 50 mL), and the solution was placed in a freezer at −20 °C. Colorless crystals of $Ba_2(O_2CCF_3)_4$(12-crown-4)$_2$ (**1**) formed after 1 day; the yield was 4.71 g, 87.1%. Compounds **2**−**7** were prepared in an analogous fashion but with toluene as the crystallizing solvent for **4** (2 mmol scale) and pyridine for **5**. Yields: 4.83 g (89.1%) (**2**), 5.17 g (84%) (**3**), 1.31 g (88%) (**4**), 6.41 g (90.7%) (**5**), 5.45 g (82.8%) (**6**), 6.27 g (95 0.3%) (**7**).

Characterization Data. $Ba_2(O_2CCF_3)_4$(12-crown-4)$_2$ (1). ^{1}H NMR ([D$_4$]methanol): 3.80 (s, $C_8H_{16}O_4$). ^{1}H NMR ([D$_4$]methanol): uncoordinated 12-crown-4, 3.66. ^{13}C NMR ([D$_4$]methanol): 67.49 (s, $C_8H_{16}O_4$), 118.2 (q, $-CF_3$, J_{C-F} = 294 Hz), 163.3 (q, C(O), $^2J_{C-F}$ = 31.7 Hz). IR (KBr, cm^{-1}): 2926 (m), 2885.8 (m), 1690 (s, $\nu_{asym}(CO_2)$), 1486 (w), 1470 (w), 1455 (m), 1441 (m), 1368 (w), 1307 (w), 1290 (m), 1248 (m), 1206 (s), 1136 (s), 1089 (s), 1053 (w), 1022 (s), 921 (m), 855 (m), 843 (m), 799 (m), 724 (m). TGA (air, 10 °C/min): 250−310 °C, 66.4% weight loss (expected 67.5% based on BaF_2 formation). Anal. Found (calcd for $Ba_2O_{16}F_{12}C_{24}H_{32}$): C, 26.50 (26.71); H, 2.81 (2.99).

$Ba_2(O_2CCF_3)_4$(triglyme)$_2$ (2). ^{1}H NMR ([D$_4$]methanol): 3.41 (s, 6H, $-OCH_3$), 3.60 (m, 4H, $-OCH_2-$), 3.67 (m, 4H, $-OCH_2-$), 3.69 (s, 4H, $-OCH_2-$). ^{1}H NMR ([D$_4$]methanol): uncoordinated triglyme, 3.35 (s, 6H, $-OCH_3$), 3.52 (m, 4H, $-OCH_2-$), 3.61 (s, 4H, $-OCH_2-$). ^{13}C NMR ([D$_4$]methanol): 59.3 (s, $-OCH_3$), 71.1 (s, $-OCH_2-$), 71.15 (s, $-OCH_2-$), 72.6 (s, $-OCH_2-$), 118.2 (q, $-CF_3$, J_{C-F} = 293 Hz), 163.4 (q, C(O), $^2J_{C-F}$ = 34.7 Hz). IR (KBr, cm^{-1}): 2948 (m), 1693 (s, $\nu_{asym}(CO_2)$), 1489 (w) 1464 (m), 1454 (m), 1434 (m), 1207 (s), 1178 (s), 1131 (s), 1085 (s), 1062 (m), 1021 (m), 982 (w), 924 (w), 861 (m), 841 (m), 798 (m), 721 (m). TGA (air, 10 °C/min): 180−370 °C, 66.9% weight loss (expected 67.6% based on BaF_2 formation). Anal. Found (calcd for $Ba_2O_{16}F_{12}C_{24}H_{36}$): C, 26.59 (26.61); H, 3.48 (3.35).

$Ba_2(O_2CCF_3)_4$(15-crown-5CH_2OH)$_2$ (3). ^{1}H NMR ([D$_4$]methanol): 3.55−3.9 (overlapping ms, $-OCH_2-$). ^{1}H NMR ([D$_4$]methanol): uncoordinated 15-crown-5CH_2OH, 3.5−3.8. ^{13}C NMR ([D$_4$]methanol): 63.2, 68.7, 69.5, 69.6, 69.65, 69.7, 70.0, 70.3, 70.4, 72.0, 79.0 (s,

(17) Zhao, J.; Marcy, H. O.; Tonge, L. M.; Wessels, B. W.; Marks, T. J.; Kannewurf, C. R. *Mater. Res. Soc. Symp. Proc.* **1990**, *169*, 593−6.
(18) Zhao, J.; Dahmen, K. H.; Marcy, H. O.; Tonge, L. M.; Wessels, B. W.; Marks, T. J.; Kannewurf, C. R. *Solid State Commun.* **1989**, *69*, 187−9.
(19) Zhang, J. M.; Wessels, B. W.; Richeson, D. S.; Marks, T. J.; DeGroot, D. C.; Kannewurf, C. R. *J. Appl. Phys.* **1991**, *69*, 2743−5.
(20) Watson, I. M.; Atwood, M. P.; Cardwell, D. A.; Cumberbatch, T. J. *J. Mater. Chem.* **1994**, *4*, 1393−1401.
(21) Spee, C. I. M. A.; Vanderzouwenassink, E. A.; Timmer, K.; Mackor, A.; Meinema, H. A. *J. Phys. 2* **1991**, *1*, 295−302.
(22) Nystrom, M. J.; Wessels, B. W.; Lin, W. P.; Wong, G. K.; Neumayer, D. A.; Marks, T. J. *Appl. Phys. Lett.* **1995**, *66*, 1726−8.
(23) Hanusa, T. P. *Chem. Rev.* **1993**, *93*, 1023−1036.
(24) Burkey, D. J.; Alexander, E. K.; Hanusa, T. P. *Organometallics* **1994**, *13*, 2773−86.
(25) Schulz, D. L.; Marks, T. J. *Adv. Mater.* **1994**, *6*, 719−730.
(26) Caruso, J.; Hampden-Smith, M.; Rheingold, A. L.; Yap, G. *J. Chem. Soc., Commun.* **1995**, *2*, 157.
(27) Caruso, J.; Hampden-Smith, M. J.; Duesler, E. *J. Chem. Soc., Chem. Commun.* **1995**, 157.
(28) Wojtczak, W.; Atanasova, P.; Duesler, E.; Hampden-Smith, M. J. *Inorg. Chem.* **1995**, *35*, 6995.
(29) Apblett, A. W.; Cubano, L. A.; Georgieva, G. D.; Mague, J. T. *Chem. Mater.* **1996**, *8*, 650.
(30) Chandler, C. D.; Roger, C.; Hampden-Smith, M. J. *Chem. Rev.* **1993**, *93*, 1205.
(31) Archer, L. Ph.D. Dissertation, **1996**.
(32) Rheingold, A. L.; White, C. B.; Haggerty, B. S.; Kirlin, P.; Gardiner, R. A. *Acta Crystallogr.* **1993**, *C49*, 808.

Table 1. Crystal and Refinement Data for **1**−**6**

	1	**2**	**3**	**4**	**5**	**6**
molecular formula	$Ba_2O_{16}F_{12}C_{24}H_{32}$	$Ba_2O_{16}F_{12}C_{24}H_{36}$	$Ba_2O_{20}F_{12}C_{30}H_{44}$	$BaN_2O_{10}F_6C_{22}H_{36}$	$BaNO_{10}F_6C_{21}H_{29}$	$BaO_{11}F_6C_{17}H_{26}$
fw	1079.2	1083.2	1227.4	739.9	706.8	657.7
cryst system	monoclinic	monoclinic	monoclinic	tetragonal	orthorhombic	monoclinic
space group	$P2_1/n$	$P2_1/n$	$P2_1/c$	$P4_32_12$	*Pnma*	*Pn*
a, Å	11.014(1)	11.203(1)	12.445(2)	a = b	27.178(3)	8.279(1)
b, Å	12.016(1)	12.220(1)	12.499(3)	9.263(2)	11.417(1)	11.410(1)
c, Å	15.269(1)	15.451(1)	15.615(2)	35.897(7)	9.133(1)	13.661(2)
β, deg	104.47(1)	107.61(1)	111.11(1)	-	-	98.41(1)
V, Å^3	1956.9(3)	2015.5(3)	2266.4(7)	3079.9(9)	2834.8(5)	1277.1(3)
Z	4	4	4	4	4	2
d_{calc}, g/cm^3	1.831	1.785	1.798	1.596	1.656	1.710
μ, mm^{-1}	2.119	2.058	1.848	1.377	1.490	1.649
T, K	293	293	293	293	293	293
cryst size, mm	0.230 × 0.253 × 0.610	0.345 × 0.368 × 0.391	0.230 × 0.346 × 0.350	0.046 × 0.138 × 0.368	0.161 × 0.368 × 0.621	0.276 × 0.460 × 0.529
reflcns collcd	11970	9229	8935	10781	15996	7685
obsd reflcns	3193 ($F > 2\sigma(F)$)	2448 ($F > 3\sigma(F)$)	3252 ($F > 2\sigma(F)$)	2598 ($F > 2\sigma(F)$)	2319 ($F > 3\sigma(F)$)	3629 ($F > 3\sigma(F)$)
no. of params	237	240	287	237	192	304
$R(F)$, %[a]	5.19	4.48	5.59	4.42	5.30	2.76
$R_w(F)$, %[b]	5.34	4.19	6.11	2.99	5.45	2.94
largest peak, e/Å^3	0.956	0.511	1.384	0.896	1.235	0.747

[a] $R = \sum\Delta F/\sum F_o$. [b] $R_w = \sum w^{1/2}\Delta F/\sum w^{1/2}F_o$; $w^{-1} = \sigma^2(F) + 0.0005F^2$.

−O*C*H$_2$−), 118.3 (q, -*C*F$_3$, J_{C-F} = 294 Hz). IR (KBr, cm^{-1}): 3316 (m), 2926 (m),1707 (s, $\nu_{asym}(CO_2)$), 1676 (s, $\nu_{asym}(CO_2)$), 1476 (m), 1457 (m), 1437 (m), 1430 (m), 1357 (m), 1205 (s), 1180 (s), 1127 (s), 1087 (s), 1059 (m), 994 (m), 942 (m), 876 (m), 842 (m), 829 (m), 799 (m), 724 (m). TGA (air, 10 °C/min): 232−335 °C, 71.1% weight loss (expected 71.4% based on BaF_2 formation). Anal. Found (calcd for $Ba_2O_{20}F_{12}C_{30}H_{44}$): C, 29.14 (29.36); H, 3.39 (3.61).

Ba(O$_2$CCF$_3$)$_2$(cryptand(222)) (4). ^{1}H NMR ([D$_3$]acetonitrile): 2.71 (t, 12H, −NC*H*$_2$−, J = 4.8 Hz), 3.66 (s, 12H, −OC*H*$_2$−), 3.74 (t, 12H, −OC*H*$_2$−, J = 4.8 Hz). ^{1}H NMR ([D$_3$]acetonitrile): uncoordinated kryptand(222), 2.55 (t, 12H, −NC*H*$_2$−, J = 5.7 Hz), 3.52 (t, 12H, −OC*H*$_2$−, J = 5.7 Hz), 3.58 (s, 12H, −OC*H*$_2$−). ^{13}C NMR ([D$_3$]acetonitrile): 54.8 (s, −NCH$_2$−), 68.9 (s, −OCH$_2$−), 71.0 (s, −OCH$_2$−), 118.7 (q, −*C*F$_3$, J_{C-F} = 298 Hz), 159.8 (q, *C*(O), $^2J_{C-F}$ = 32.0 Hz). IR (KBr, cm^{-1}): 2924 (m), 1694 (s, $\nu_{asym}(CO_2)$), 1490 (m), 1457 (m), 1448 (m), 1406 (m, $\nu_{sym}(CO_2)$), 1360 (m), 1258 (w), 1199 (s), 1170 (s), 1114 (s), 1094 (s), 1078 (m), 950 (m), 923 (w), 821 (w), 797 (w), 716 (w). TGA (air, 10 °C/min): 235−480 °C, 75.8% weight loss (expected, 76.3% based on BaF_2 formation). Anal. Found (calcd for $BaN_2O_{10}F_6C_{22}H_{36}$): C, 35.53 (35.71); H, 5.27 (4.90), N, 3.72 (3.79).

Ba(O$_2$CCF$_3$)$_2$(18-crown-6)(py) (5). ^{1}H NMR ([D$_4$]methanol): 3.77 (s, 24H, $C_{12}H_{24}O_6$), 7.40−7.46, 7.81−7.89, 8.51−8.54, (ms, 5H, C_5H_5N). ^{1}H NMR ([D$_4$]methanol): uncoordinated 18-crown-6, 3.63. ^{13}C NMR ([D$_4$]methanol): 71.3 (s, −OCH$_2$−), 118.5 (q, −*C*F$_3$, J_{C-F} = 299 Hz), 125.6, 138.4, 150.1 (s, C_5H_5N). IR (KBr, cm^{-1}): 2927 (m), 2894 (m), 1700 (s, $\nu_{asym}(CO_2)$), 1678 (s, $\nu_{asym}(CO_2)$), 1477 (m), 1450 (m), 1427 (m), 1415 (w), 1354 (m), 1305 (w), 1291 (w), 1253 (m), 1206 (s), 1169 (s), 1104 (s), 1034 (m), 962 (s), 872 (w), 834 (m), 800 (m), 760 (w). TGA (air, 10 °C/min): 100 °C, 11% weight loss (−pyridine, calcd weight loss 11.2%), 260−300 °C, 74.2% weight loss (expected, 75.2% based on BaF_2 formation). Anal. Found (calcd for $BaNO_{10}F_6C_{21}H_{29}$): C, 34.47 (35.69); H, 4.15 (4.14); N, 1.54 (1.98).

Ba(O$_2$CCF$_3$)$_2$(18-crown-6CH$_2$OH) (6). ^{1}H NMR ([D$_3$]acetonitrile): 3.5−4.1 (overlapping ms, 26H, −OC*H*$_2$−), 6.18 (br s, −O*H*). ^{1}H NMR ([D$_3$]acetonitrile): uncoordinated 18-crown-6CH$_2$OH, 3.44−3.75 (overlapping ms, 26H, −OC*H*$_2$−), 2.24 (br s, −O*H*). ^{13}C NMR ([D$_3$]acetonitrile): 59.6, 68.2, 70.2, 70.4, 70.5, 70.6, 71.0, 71.25, 71.3, 71.4, 75.2, 78.3 (s, −OCH$_2$−), 118.4 (q, −*C*F$_3$, J_{C-F} = 298 Hz), 161.8 (q, *C*(O), $^2J_{C-F}$ = 33 Hz). IR (KBr, cm^{-1}): 3382 (m), 2924 (m), 1695 (s, $\nu_{asym}(CO_2)$), 1669 (s, $\nu_{asym}(CO_2)$), 1474 (m), 1457 (w), 1434 (m), 1420 (w), 1353 (m), 1289 (w), 1250 (w), 1204 (s), 1180 (s), 1094 (s), 996 (m), 964 (m), 954 (m), 902 (w), 830 (m), 828 (m), 802 (m), 723 (m). TGA (air, 10 °C/min): 210−320 °C, 71.8% weight loss (expected, 73.3% based on BaF_2 formation). Anal. Found (calcd for $BaO_{11}F_6C_{17}H_{26}$): C, 31.22 (31.04); H, 4.19 (3.98).

Ba(O$_3$SCF$_3$)$_2$(tetraglyme) (7). ^{1}H NMR ([D$_4$]methanol): 3.42 (s, 6H, −OC*H*$_3$), 3.60−3.63 and 3.68−3.71 (ms, 16H, −OC*H*$_2$−). ^{1}H NMR ([D$_4$]methanol): uncoordinated tetraglyme, 3.35 (s, 6H, −OC*H*$_3$), 3.51−3.54 and 3.60−3.63 (m, 16H, −OC*H*$_2$−). ^{13}C NMR ([D$_4$]-methanol): 59.5 (s, −OCH$_3$), 70.8, 71.1, 72.2 (s, −OCH$_2$−), 121.7 (q, −*C*F$_3$, J_{C-F} = 319 Hz). IR (KBr, cm^{-1}): 2933 (m), 1496 (w), 1473 (w), 1457 (w), 1399 (w), 1351 (w), 1288 (s), 1256 (s), 1230 (s), 1182 (m), 1155 (m), 1093 (m), 1041 (s), 1019 (w), 949 (m), 873 (w), 851 (w), 827 (w), 759 (w). TGA (air, 10 °C/min): 190−255 °C, 35.0% weight loss (−tetraglyme, calcd weight loss 33.8%), 500−620 °C, 73.3% weight loss (expected, 73.3% weight loss based on BaF_2 formation). Anal. Found (calcd for $BaS_2O_{11}F_6C_{12}H_{22}$): C, 21.70 (21.91); H, 3.63 (3.37).

X-ray Crystallography. Data for **1**−**6** were collected on a Siemens R3m/V automated diffractometer with graphite-monochromated Mo Kα radiation (λ = 0.710 73 Å). The unit cells were determined by using search, center, index, and least-squares routines. The Laue classes and cell dimensions were confirmed by axial oscillation photography. In each case, the data were corrected for Lorentz and polarization effects and an anisotropic decay correction was also applied on the basis of the measurement of 3 check reflections after every 97 data. Semiempirical absorption corrections based on ψ-scans were also applied.

Each structure was solved by the Patterson method using the Siemens SHELXTL Plus program software for all computations (G. Sheldrick, Siemens XRD, Madison, WI). Crystallographic data and the results of structure refinements for **1**−**6** are provided in Table 1. Positional parameters and equivalent isotropic thermal parameters were deposited as Supporting Information.

Compound **1** crystallized from ethanol as colorless prisms in the monoclinic crystal system. The space group $P2_1/n$ was uniquely defined from the systematic absences. **1** resides on an inversion center in the unit cell. The barium, carbon and oxygen atoms were refined anisotropically except for C(4) of the 12-crown-4 ring which was disordered over two positions. C(4) and C(4′) were refined isotropically with fixed occupancies of 52.5% and 47.5%, respectively. A 2-fold rotational disorder in the −CF$_3$ groups resulted in refinement of the fluorine atoms with fixed occupancies (F_{1-3}, 61.7%; F_{4-6}, 60.2%) and variable isotropic displacement coefficients (U's). Hydrogen atom positions were calculated by a riding model with set isotropic displacement coefficient of 1.25 times U_{eq} of the corresponding carbon atom.

Compound **2** crystallized from ethanol as colorless blocks in the monoclinic space group $P2_1/n$. Compounds **1** and **2** are isotypic as can be seen from their unit cell parameters in Table 1 and their structures shown in Figures 1 and 2. Compound **2** resides on an inversion center in the unit cell. A 2-fold rotational disorder in one −CF$_3$ group and a 3-fold disorder in the other −CF$_3$ group resulted in refinement of the fluorine atoms with fixed occupancies (F_{1-3}, 50.8%; F_{4-6}, 48.0%, $F_{4-6'}$, 26.0%, $F_{4-6''}$, 26.0%). Atoms O(1), C(1), C(2), C(6), and C(7) of the

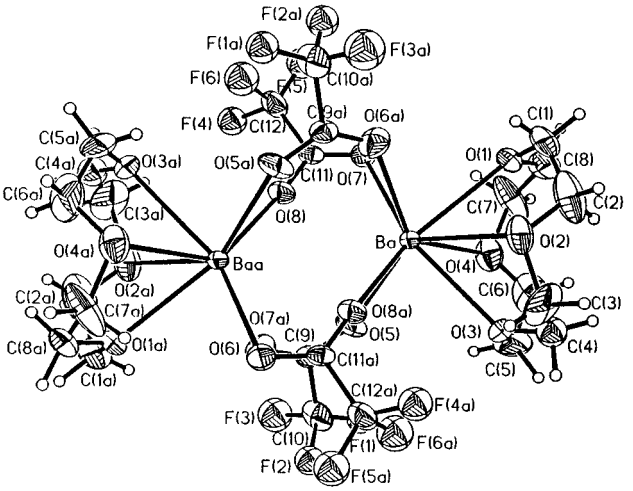

Figure 1. ORTEP plot of $Ba_2(O_2CCF_3)_4$(12-crown-4)$_2$ (**1**). Only one orientation of disordered atoms is shown. Thermal ellipsoids are scaled to the 20% probability level except for hydrogen atoms which have been given arbitrary thermal parameters for clarity.

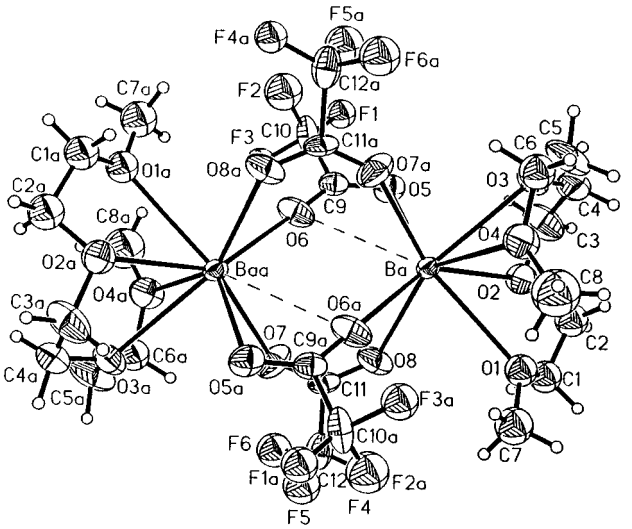

Figure 2. ORTEP plot of $Ba_2(O_2CCF_3)_4$(triglyme)$_2$ (**2**). Only one orientation of disordered atoms is shown. Thermal ellipsoids are scaled to the 20% probability level except for hydrogen atoms which have been given arbitrary thermal parameters for clarity.

triglyme ligand were disordered over two sites and refined isotropically with fixed occupancies of 69.5%, 69.5%, 69.5%, 50%, and 69.5%, respectively. Although no alternate sites could be located for C(8), it had large anisotropic displacement coefficients and was, therefore, refined isotropically. The barium atom and remaining carbon and oxygen atoms were refined anisotropically. Geometrically constrained hydrogen atoms were placed in calculated positions with their isotropic displacement coefficients set to 1.25 times U_{eq} of the corresponding carbon atom. Additional information on the disorder model for this compound is provided in Supporting Information.

Compound **3** crystallizes from ethanol as colorless plates in the monoclinic space group $P2_1/c$. Compound **3** resides on an inversion center in the unit cell. Fluorine atoms associated with C(13) are disordered over two positions and were constrained with C−F = 1.33 Å and F−F′ = 2.19 Å. The disordered fluorine atoms were initially refined with a common isotropic displacement coefficient. The occupancies converged to 66.7% for F(1)−F(3) and 33.3% for F(1′)−F(3′). The final model had anisotropic refinement on all other non-hydrogen atoms and isotropic refinement of the disordered fluorine atoms with fixed occupancies and variable U's. Hydrogen atoms, other than the hydroxyl proton of O(6), were placed in idealized positions with set isotropic displacement coefficient of 1.25 times U_{eq} of the corresponding carbon atom. The hydroxyl proton of O(6) was fixed at 0.85 Å from O(6) along a vector to O(8A), which places it in a good position for hydrogen bonding. The isotropic U was allowed to vary and refined to a value of 0.089(40) Å^2.

Compound **4** crystallizes from toluene as transparent plates in the tetragonal polar space group $P4_32_12$. Molecules of **4** reside on crystallographic 2-fold axes, which pass through the barium atoms and bisect the C(3)−C(3a) bonds and the N−Ba−N(Oa) angles. The fluorine atoms of the $-CF_3$ groups of **4** were disordered over two positions and refined isotropically with site occupancies of 55.0% (F(1)−F(3)) and 45% (F(1′)−F(3′)). All other non-hydrogen atoms were refined anisotropically. Hydrogen atoms were included in calculated positions with set U's of 1.25 times U_{eq} of the corresponding carbon atom. The final model was tested for handedness. The inverted model in $P4_12_12$ showed slightly higher R values. The accepted model was the original in space group $P4_32_12$.

Compound **5** crystallized from pyridine as transparent prisms in the orthorhombic space group *Pnma*. The molecule has a crystallographic mirror plane which bisects the Ba, O(1), O(4), O(6), O(7), C(7)−C(10), C(13), F(1), F(1′), and N atoms. The fluorine atoms of both $-CF_3$ groups are rotationally disordered over two sites. The fluorine atoms of C(8) have site occupancies of 32.5% (F(1)), 65% (F(2)), 17.5 (F(1′)), and 35% (F(2′)). These occupancies were obtained by constraining the isotropic U's to be equal. The fluorine atoms of C(10) do not reside on the mirror plane and were, therefore, assigned occupancies of 50%. The $-CF_3$ groups were refined with C−F and F−F distances constrained to 1.34 and 2.19 Å, respectively. All non-hydrogen and non-fluorine atoms were refined anisotropically in the final model with hydrogen atoms in idealized positions with set U's of 1.25 times U_{eq} of the corresponding carbon atom. The fluorine atoms were refined in the final model with fixed occupancies and variable U's.

Compound **6** crystallizes from ethanol as colorless blocks in the polar monoclinic space group *Pn*. The fluorine atoms of C(17) are disordered over two sites with occupancies of 55.05% (F(4)−F(6)) and 44.95% (F(4′)−F(6′)). The hydroxyl methylene group is also disordered over two sites, one at C(1) (C(13), O(7), and H(7)) 65.64% of the time and the other at C(12) (C(13′), O(7′), and H(7′)) 34.36% of the time. The final model included these disordered atoms with fixed occupancies and variable U's. All other non-hydrogen atoms were refined anisotropically with hydrogen atoms included in idealized positions. H(7) was placed at a reasonable hydrogen bonding position approximately 1.8 Å from O(11) and 0.92 Å from O(7) (O(7′)). The inverted model was also tested in space group *Pn* with poorer results. The reported structure reflects the original model for which the R-values were lower.

Results and Discussion

Synthesis. Reaction of BaH_2 with polydentate neutral ligands and strong acids such as CF_3COOH or CF_3SO_3H in 1:1:2 stoichiometries, in THF as solvent, yielded a series of mononuclear and dinuclear polydentate ligand adducts of barium trifluoroacetate and trifluoromethanesulfonate. The reactions with BaH_2 provide a clean route to anhydrous trifluoroacetate compounds. The driving force in the reactions appears to be the formation of H_2 gas and the salt of the conjugate base BaX_2L ($X = CF_3CO_2^-$, $CF_3SO_3^-$; L = 12-crown-4 (**1**), triglyme (**2**), 15-crown-5CH_2OH (**3**), cryptand(222) (**4**), 18-crown-6·C_5H_5N (**5**), 18-crown-6CH_2OH (**6**), and tetraglyme (**7**)). A similar reaction has been employed in the synthesis of polyether adducts of group 2 β-diketonates.[1] An alternate route to compounds of formula BaX_2L is reaction of $BaCO_3$ or $Ba(OH)_2$ with acid and polydentate ligand. However, this route is not anhydrous or very useful for weaker acids. For example, we have found that acetic acid does not react appreciably over a 1-day period with $BaCO_3$ and polyether in ethanol or other nonaqueous solvents such as THF or toluene.

For each of the above compounds, a 1:1 (M:L) adduct is formed to give low nuclearity trifluoroacetate adducts with metal coordination numbers between 8 and 10. The solubilities of compounds **1**−**7** as well as other group 2 metal carboxylate

Table 2. Barium Carboxylate and Sulfonate Polydentate Ligand Adducts and Their Physical Properties[a]

compd	ν (CO_2) (asym), cm^{-1}	carboxylate bonding mode[b]	CN	solubility[f]	thermal dec prod (air)	ref(s)
[Ba(pivalate)(dicyclohexano-18-crown-6)(H_2O)$_2$](pivalate)(H_2O)	*	dangling, **I**, ionic	9	s = a/b	*	38
Ba(pivalate)$_2$(18-crown-6)	*	chelating, **II**	10	s = c	*	32
[Ba(adipate)$_2$(18-crown-6)·8H_2O]$_\infty$	*	chelating, **II**	10	s = a; ss = b; is = c	$BaCO_3$	31
Ba(O_2CCH_3)$_2$(18-crown-6)·1.5H_2O	*	*	*	s = a/b	*	31
Ba(O_2CCH_3)$_2$(18-crown-6)·4H_2O	1560	chelating,[c] **II**	10	s = a; ss = b; is = c	$BaCO_3$	31
Ba(O_2CCF_3)$_2$·THF	1662	*	*	s = b, d	BaF_2	this work
Ba(O_2CCF_3)$_2$(18-crown-6)·H_2O	*	*	*	*	*	39
Ba$_2$(O_2CCF_3)$_4$(12-crown-4)$_2$ (**1**)	1690	bridging, **VI** and **VII**	8−9	s = a, b; ss = d; is = c	BaF_2	this work
Ba$_2$(O_2CCF_3)$_4$(triglyme)$_2$ (**2**)	1693	bridging, **VI** and **VII**	8−9	s = a, b; ss = d	BaF_2	this work
Ba$_2$(O_2CCF_3)$_4$(15-crown-5)$_2$	1717	bridging, **VI**	9	s = a, b; ss = d; is = c	BaF_2	28
Ba$_2$(O_2CCF_3)$_4$(15-crown-5CH_2OH)$_2$ (**3**)	1707 1676	bridging, **VI** chelating,[d] **II**	9−10	s = b	BaF_2	this work
Ba(O_2CCF_3)$_2$(cryptand(222)) (**4**)	1694	dangling, **I**	10	s = b, c, g	BaF_2	this work
Ba(O_2CCF_3)$_2$(18-crown-6)(py) (**5**)	1700 1678	dangling, **I** chelating, **II**	10	s = e	BaF_2	this work
Ba(O_2CCF_3)$_2$(18-crown-6CH_2OH) (**6**)	1695 1669	dangling,[e] **I** chelating, **II**	10	s = a, b	BaF_2 and $BaCO_3$	this work
[Ba$_2$(O_2CCF_3)$_4$(tetraglyme)]$_\infty$	1686 1655	bridging, **VI** chelating/bridging, **IX**	9	s = b, d, f; ss = c	BaF_2	28
Ba(O_3SCF_3)$_2$	*	*	*	*	*	32
Ba(O_3SCF_3)$_2$(18-crown-6)·H_2O	*	*	*	*	*	32
Ba(O_3SCF_3)$_2$(tetraglyme) (**7**)	1288, 1256 (S=O)	*	*	s = b	BaF_2	this work

[a] Asterisk = not available. [b] Refer to Chart 1 for bonding mode diagrams. [c] Water molecules are hydrogen bonded to carboxylate ligands. [d] Weakly chelating, involved in intramolecular hydrogen bonding. [e] Trifluoroacetate ligand involved in intermolecular hydrogen bonding. [f] s = soluble, ss = slightly soluble, is = insoluble; a = water, b = alcohols, c = toluene, d = tetrahydrofuran, e = pyridine, f = acetonitrile.

adducts are given in Table 2. Compounds **1**−**7** all have good solubility in alcohols and water. Compound **4** and Ba(pivalate)$_2$-(18-crown-6)[30] are among the few compounds that are soluble in noncoordinating solvents such as toluene. A larger group (**1**−**3**) and ([M_2(O_2CCF_3)$_4$(tetraglyme)]$_\infty$, M = Sr, Ba)[28] show slight to good solubility in THF. Compounds **1**−**6** do not sublime intact when heated under vacuum (200 °C, 10^{-4} Torr). Instead, the polydentate ligand is released leaving barium trifluoroacetate (sulfonate) behind. These species are, therefore, unlikely to be suitable for transport of Ba using conventional delivery for CVD;[33] however, this does not rule out the use of other delivery methods such as liquid delivery[34] or aerosol delivery.[33,35]

Structures. Compounds **1** and **2** have similar structures with four bridging trifluoroacetate ligands and side-on bonding of the polyether ligands as shown in Figures 1 and 2, respectively. Selected listings of bond distances and angles for **1** and **2** are given in Tables 3 and 4, respectively. The bonding mode(s) of the trifluoroacetate ligands are assigned in Table 2 in accordance with Chart 1, which shows the variety of bonding modes that have been described for metal carboxylate complexes in general.[36] Both compounds are quite similar to the previously reported Ba$_2$(O_2CCF_3)$_4$(15-crown-5)$_2$.[28] These three compounds have polyethers in common that are too small to encapsulate the barium atom at its midpoint and prefer to sit to one side of the metal center. This behavior has also been observed in the group 2 β-diketonate compounds with these ethers.[1] This side-on bonding opens up the opposite side of the metal atom to the bridging trifluoroacetate ligands. There are, however, some differences in the structures of the three compounds. Whereas

Table 3. Selected Listing of Bond Distances (Å) and Bond Angles (deg) for **1**

Bond Distances			
Ba−O(1)	2.807(7)	Ba−O(2)	2.824(8)
Ba−O(3)	2.773(8)	Ba−O(4)	2.855(7)
Ba−O(5)	2.701(7)	Ba−O(7)	2.790(6)
Ba···Baa	4.195(1)	Ba−O(6a)	2.699(7)
Ba−O(8a)	2.683(5)		
Bond Angles			
O(1)−Ba−O(3)	86.0(2)	O(2)−Ba−O(4)	89.4(2)
O(1)−Ba−O(5)	139.1(2)	O(2)−Ba−O(5)	135.0(2)
O(3)−Ba−O(5)	79.6(2)	O(4)−Ba−O(5)	81.2(2)
O(1)−Ba−O(7)	75.5(2)	O(2)−Ba−O(7)	130.1(2)
O(3)−Ba−O(7)	140.7(2)	O(4)−Ba−O(7)	81.8(2)
O(5)−Ba−O(7)	92.1(2)	O(1)−Ba−O(6a)	79.8(2)
O(2)−Ba−O(6a)	79.4(2)	O(3)−Ba−O(6a)	136.6(2)
O(4)−Ba−O(6a)	136.1(3)	O(5)−Ba−O(6a)	134.8(2)
O(7)−Ba−O(6a)	74.1(2)	O(8)−Ba−O(6a)	68.4(2)
O(2)−Ba−O(8a)	86.2(2)	O(1)−Ba−O(8a)	143.0(2)
O(4)−Ba−O(8a)	138.3(2)	O(3)−Ba−O(8a)	83.9(2)
O(7)−Ba−O(8a)	130.6(2)	O(5)−Ba−O(8a)	73.3(2)
Ba−O(5)−C(9)	137.2(5)	O(8)−Ba−O(8a)	87.4(2)
Ba−O(7)−C(11)	100.0(5)	O(6a)−Ba−O(8a)	83.5(2)
Baa−O(6)−C(9)	131.7(7)	Baa−O(8)−C(11)	164.4(5)
Ba−O(8)−Baa	92.6(2)		

the bonding of the bridging trifluoroacetate ligands in Ba$_2$(O_2-CCF_3)$_4$(15-crown-5)$_2$ is roughly symmetrical with Ba−O_{acet} bond distances in the range of 2.635(14)−2.652(11) Å, the same ligands in **1** and **2** show some asymmetry in their bonding with wider variation in bond distance ranges of 2.685(5)−2.790(6) and 2.648(8)−2.763(7) Å, respectively. The barium atoms of **1** and **2**, as indicated in Figures 1 and 2, each have an additional long Ba−O_{acet} bridging interaction (3.104(6) Å (Ba−O(8)) for **1** and 3.298(8) Å (Ba−O(6) for **2**) from a μ_2-oxygen atom of a trifluoroacetate ligand. These long interactions are undoubtedly the reason for the distorted structures of **1** and **2** as compared to Ba$_2$(O_2CCF_3)$_4$(15-crown-5)$_2$, and the large differences in the Ba−Ba contacts of 4.735(1) Å for Ba$_2$(O_2CCF_3)$_4$(15-crown-5)$_2$ and 4.195(1) and 4.380(1) Å for **1** and **2**, respectively, lends support to this view. The distortion in **1** and **2** can also be

(33) Kodas, T. T.; Hampden-Smith, M. J. In *The Chemistry of Metal CVD; Chapter 9*; Kodas, T. T., Hampden-Smith, M. J., Eds.; VCH: Weinheim, Germany, 1994; Chapter 9.
(34) Van Buskirk, P. C.; Gardiner, R. A.; Kirlin, P. S.; Nutt, S. *J. Mater. Res.* **1992**, *7*, 542.
(35) Xu, C.; Kodas, T. T.; Hampden-Smith, M. J. *Chem. Mater.* **1995**, *7*, 1539−1546.
(36) Deacon, G. B.; Phillips, R. J. *Coord. Chem. Rev.* **1980**, *33*, 227.

Table 4. Selected Listing of Bond Distances (Å) and Bond Angles (deg) for **2**[a]

Bond Distances			
Ba−O(1)	2.883(11)	Ba−O(1′)	2.845(24)
Ba−O(2)	2.850(6)	Ba−O(3)	2.862(9)
Ba−O(4)	2.857(8)	Ba−O(5)	2.763(7)
Ba−O(6)	3.298(8)	Ba−O(8)	2.702(9)
Ba−O(6a)	2.648(8)	Ba−O(7a)	2.655(7)
Ba···Baa	4.380(1)		

Bond Angles			
O(1)−Ba−O(3)	89.5(3)	O(1′)−Ba−O(3)	91.9(5)
O(2)−Ba−O(4)	96.0(2)	O(1)−Ba−O(5)	130.9(2)
O(1′)−Ba−O(5)	153.3(4)	O(2)−Ba−O(5)	77.4(2)
O(3)−Ba−O(5)	75.9(2)	O(4)−Ba−O(5)	127.2(3)
O(1)−Ba−O(6)	146.0(3)	O(1′)−Ba−O(6)	155.6(6)
O(2)−Ba−O(6)	113.1(2)	O(3)−Ba−O(6)	112.2(2)
O(4)−Ba−O(6)	137.6(2)	O(5)−Ba−O(6)	41.5(2)
O(1)−Ba−O(8)	71.9(3)	O(11)−Ba−O(8)	84.1(6)
O(2)−Ba−O(8)	83.4(2)	O(3)−Ba−O(8)	140.9(2)
O(4)−Ba−O(8)	141.3(3)	O(5)−Ba−O(8)	90.6(3)
O(6)−Ba−O(8)	74.9(2)	O(1′)−Ba−O(6a)	76.3(5)
O(1)−Ba−O(6a)	92.2(3)	O(3)−Ba−O(6a)	142.8(2)
O(2)−Ba−O(6a)	145.6(2)	O(5)−Ba−O(6a)	127.2(2)
O(4)−Ba−O(6a)	86.7(3)	O(8)−Ba−O(6a)	73.8(2)
O(6)−Ba−O(6a)	85.7(2)	O(1′)−Ba−O(7a)	125.3(5)
O(1)−Ba−O(7a)	147.5(3)	O(3)−Ba−O(7a)	81.4(3)
O(2)−Ba−O(7a)	136.1(3)	O(5)−Ba−O(7a)	77.0(2)
O(4)−Ba−O(7a)	72.8(2)	O(8)−Ba−O(7a)	131.6(3)
O(6)−Ba−O(7a)	64.8(2)	Ba−O(6)−C(9)	81.4(6)
O(6a)−Ba−O(7a)	77.4(3)	Baa−O(6)−C(9)	171.8(8)
Ba−O(5)−C(9)	107.3(7)	Ba−O(8)−C(11)	129.2(6)
Ba−O(6)−Baa	94.3(2)	Baa−O(7)−C(11)	143.3(9)

[a] Primed atoms represent alternate positions for unprimed atoms.

Chart 1

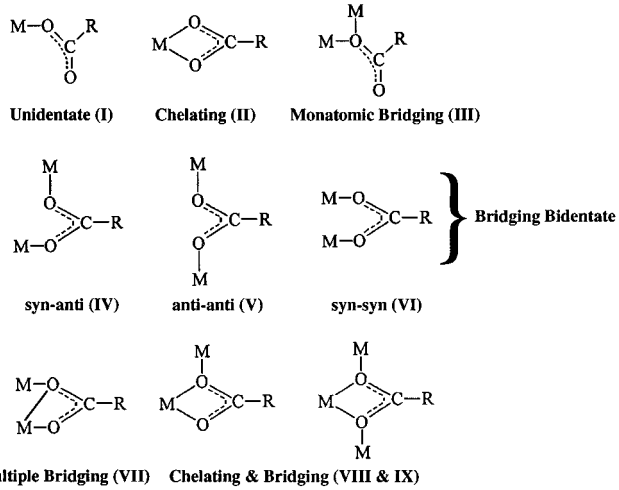

detected in the Ba−O_{acet}−C angles which have a range of 100.0(5)−164.4(5) and 107.3(7)−171.8(8)°, respectively. The range of the Ba−O_{acet}−C angles in $Ba_2(O_2CCF_3)_4$(15-crown-5)$_2$ is a relatively narrow 135.4(11)−142.2(10)°. The Ba−O_{ether} bond distances and O_{acet}−C−O_{acet} bond angles of all three compounds are quite similar. The distorted structures of compounds **1** and **2** may arise from a desire to achieve a coordination number of 9 which is available to $Ba_2(O_2CCF_3)_4$-(15-crown-5)$_2$ through "normal" coordination of the ether and trifluoroacetate ligands to the metal center.

Compound **3** is dinuclear in the solid state with 15-crown-5CH_2OH ligands bonded in a side-on fashion through all five ether oxygen atoms and the hydroxy group as shown in Figure 3. A selected listing of bond distances and angles is provided in Table 5. The trifluoroacetate ligands are bonded in both bridging and chelating modes with three types of Ba−O_{acet} bond

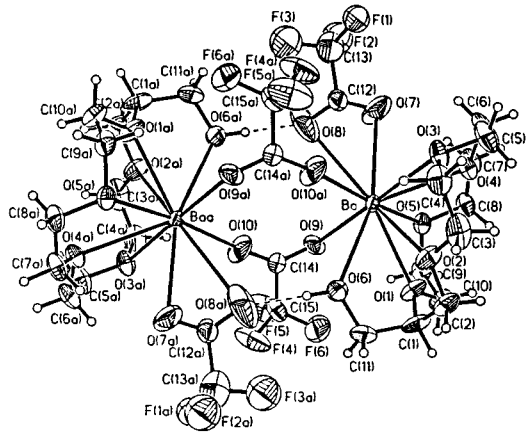

Figure 3. Molecular structure of $Ba_2(O_2CCF_3)_4$(15-crown-5CH_2OH)$_2$ (**3**). Only one orientation of disordered atoms is shown. Thermal ellipsoids are scaled to the 30% probability level except for hydrogen atoms which have been given arbitrary thermal parameters for clarity. A likely hydrogen bonding interaction is indicated by dashed line.

Table 5. Selected Listing of Bond Distances (Å) and Bond Angles (deg) for **3**

Bond Distances			
Ba−O(1)	2.762(6)	Ba−O(2)	2.930(8)
Ba−O(3)	2.945(8)	Ba−O(4)	2.948(7)
Ba−O(5)	2.962(6)	Ba−O(6)	2.844(6)
Ba−O(7)	2.813(10)	Ba−O(8)	3.266(20)
Ba−O(9)	2.726(8)		
Ba−O(10a)	2.642(8)		

Bond Angles			
O(1)−Ba−O(3)	105.7(2)	O(1)−Ba−O(4)	83.4(2)
O(2)−Ba−O(4)	82.0(2)	O(2)−Ba−O(5)	104.7(2)
O(3)−Ba−O(5)	111.0(2)	O(2)−Ba−O(6)	57.2(3)
O(1)−Ba−O(6)	58.2(2)	O(4)−Ba−O(6)	133.7(2)
O(3)−Ba−O(6)	107.2(2)	O(1)−Ba−O(7)	140.9(3)
O(5)−Ba−O(6)	111.0(2)	O(3)−Ba−O(7)	75.8(3)
O(2)−Ba−O(7)	131.6(4)	O(5)−Ba−O(7)	85.2(3)
O(4)−Ba−O(7)	64.7(3)	O(1)−Ba−O(8)	144.7(3)
O(6)−Ba−O(7)	160.2(3)	O(3)−Ba−O(8)	106.8(3)
O(2)−Ba−O(5)	155.7(3)	O(5)−Ba−O(8)	97.7(3)
O(4)−Ba−O(8)	103.5(2)	O(7)−Ba−O(8)	40.5(4)
O(6)−Ba−O(8)	122.8(3)	O(2)−Ba−O(9)	123.0(2)
O(1)−Ba−O(9)	75.3(2)	O(4)−Ba−O(9)	126.6(2)
O(3)−Ba−O(9)	177.2(2)	O(6)−Ba−O(9)	70.9(2)
O(5)−Ba−O(9)	71.8(2)	O(8)−Ba−O(9)	73.0(3)
O(7)−Ba−O(9)	105.2(3)	O(1)−Ba−O(10a)	132.8(2)
O(2)−Ba−O(10a)	87.2(3)	O(3)−Ba−O(10a)	74.3(3)
O(4)−Ba−O(10a)	126.5(3)	O(5)−Ba−O(10a)	168.0(3)
O(6)−Ba−O(10a)	76.4(2)	O(7)−Ba−O(10a)	85.9(3)
O(8)−Ba−O(10a)	70.3(3)	O(9)−Ba−O(10a)	103.0(3)
Ba−O(8)−C(12)	84.4(12)	Ba−O(6)−C(11)	121.0(6)
Baa−O(10)−C(14)	151.4(9)	Ba−O(7)−C(12)	106.4(9)
Ba−O(9)−C(14)	136.0(7)		

distances. The bridging Ba−O_{acet} bond distances have a range of 2.642(8)−2.726(8) Å, and the chelating trifluoroacetate ligand has a typical Ba−O_{acet} bond distance of 2.813(10) Å through one oxygen atom and a very long interaction of 3.266(20) Å through the other. The long interaction (Ba−O(8)) is suggestive of a possible hydrogen bonding interaction to the hydroxyl proton of O(6) which appears to be appropriately situated. The Ba−O_{ether} bond distances are of two distinct types, a short bond distance of 2.762(6) Å for Ba−O(1) and four longer distances with an average value of 2.946[11] Å. The short bond distance is associated with the ether oxygen atom of the ring closest to the hydroxy group and may arise from both a chelating effect with the Ba−O(6) hydroxy bond (2.844(6) Å) and the presence of a hydrogen bond to O(8a). Interestingly, the addition of the hydroxymethylene group to the 15-crown-5 ring results in only

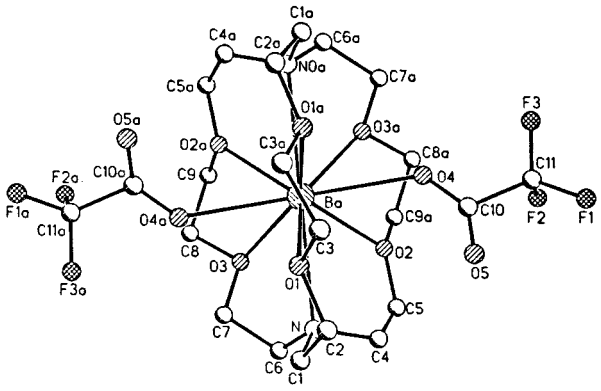

Figure 4. Molecular structure of $Ba(O_2CCF_3)_2$(cryptand(222)) (**4**) viewed down the crystallographic 2-fold axis. Only one orientation of disordered fluorine atoms is shown. Thermal ellipsoids are scaled to the 20% probability level, and hydrogen atoms have been omitted for clarity.

Table 6. Selected Listing of Bond Distances (Å) and Bond Angles (deg) for **4**

	Bond Distances		
Ba−N	2.963(4)	Ba−O(1)	2.812(5)
Ba−O(2)	2.818(4)	Ba−O(3)	2.864(3)
Ba−O(4)	2.778(5)		
	Bond Angles		
N(Oa)−Ba−N	175.8(2)	N−Ba−O(1)	62.2(1)
N−Ba−O(2)	58.7(1)	N−Ba−O(3)	59.7(1)
N−Ba−O(4)	94.3(1)	N−Ba−O(1a)	122.0(1)
N−Ba−O(2a)	118.4(1)	N−Ba−O(3a)	117.1(1)
N−Ba−O(4a)	87.0(1)	Ba−O(4)−C(10)	137.8(4)
O(1)−Ba−O(4)	80.2(1)	O(1)−Ba−O(4a)	67.8(1)
O(2)−Ba−O(4)	67.4(1)	O(2)−Ba−O(4a)	139.2(1)
O(3)−Ba−O(4)	140.3(1)	O(3)−Ba−O(4a)	70.2(1)
O(4)−Ba−O(4a)	143.1(2)	O(1)−Ba−O(1a)	60.5(1)
O(2)−Ba−O(2a)	107.8(2)	O(3)−Ba−O(3a)	94.1(2)

a partial structural change from that of $Ba_2(O_2CCF_3)_4$(15-crown-5)$_2$. The dinuclear structure is retained in **3** with two trifluoroacetate ligands bridging the barium centers, but two other trifluoroacetate ligands switch from bridging in $Ba_2(O_2CCF_3)_4$-(15-crown-5)$_2$ to chelating in **3**. This structural change allows the hydroxy group of the 15-crown-5CH_2OH ligand in **3** to bond to the metal center.

Compound **4** is mononuclear in the solid state with two dangling trifluoroacetate ligands (bonding mode **I**) and a cryptand ligand bonded to the barium atom through all six ether oxygen atoms and both nitrogen atoms to give a metal coordination number of 10. The eight coordinating oxygen atoms form a highly distorted square antiprism which is capped on the square faces by the cryptand nitrogen atoms. This compound represents the first structurally confirmed example of a purely monodentate carboxylate of a group 2 metal. Clearly, the steric effects of the ether chains of the cryptand preclude the trifluoroacetate ligands from chelating the barium center. The barium atom is roughly centered in the cryptand cavity as shown in Figure 4. A selected listing of bond distances and angles are given in Table 6. The Ba−O_{acet}, Ba−N, and Ba−O_{ether} bond distances of 2.778(5), 2.963(4), and 2.831[23] Å, respectively, are nonexceptional, and the C−O bond distances of the trifluoroacetate ligand are similar at 1.194(9) and 1.221-(8) Å. In a related barium cryptand compound, [$Ba(H_2O)_2$-(cryptand(222B)]$(Cl)_2(H_2O)_4$,[37] neither anionic ligand is bonded to the metal atom; however, oxygen atoms of two nearby water molecules are at bonding distances to the barium atom to give a metal coordination number of 10.

(37) Pettit, W. A.; Baenziger, N. C. *Acta Crystallogr.* **1994**, *C50*, 221.

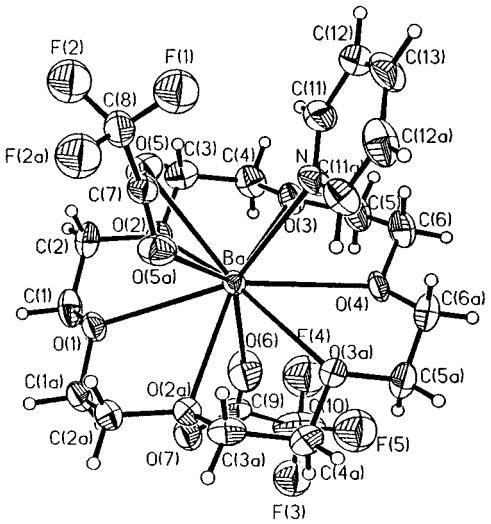

Figure 5. Molecular structure of $Ba(O_2CCF_3)_2$(18-crown-6)(py) (**5**). Only one orientation of disordered atoms is shown. Thermal ellipsoids are scaled to the 20% probability level except for hydrogen atoms which have been given arbitrary thermal parameters for clarity.

Table 7. Selected Listing of Bond Distances (Å) and Angles (deg) for **5**

	Bond Distances		
Ba−O(1)	2.845(7)	Ba−O(2)	2.820(5)
Ba−O(3)	2.854(5)	Ba−O(4)	2.869(7)
Ba−O(5)	2.877(6)	Ba−O(6)	2.631(9)
Ba−N	2.934(8)		
	Bond Angles		
O(l)−Ba−O(4)	152.3(2)	O(l)−Ba−O(5)	74.3(2)
O(2)−Ba−O(5)	71.6(l)	O(3)−Ba−O(5)	89.7(2)
O(4)−Ba−O(5)	130.5(2)	O(l)−Ba−O(6)	76.8(3)
O(2)−Ba−O(6)	73.9(l)	O(3)−Ba−O(6)	84.2(2)
O(4)−Ba−O(6)	75.5(3)	O(5)−Ba−O(6)	142.9(2)
O(l)−Ba−N	138.2(2)	O(2)−Ba−N	119.0(1)
O(3)−Ba−N	77.6(l)	O(4)−Ba−N	69.5(2)
O(5)−Ba−N	67.2(2)	O(6)−Ba−N	145.0(3)
O(3)−Ba−O(2a)	157.9(l)	O(5)−Ba−O(2a)	109.8(2)
O(6)−Ba−O(2a)	73.9(l)	N−Ba−O(2a)	119.0(1)
O(5)−Ba−O(3a)	130.4(l)	O(6)−Ba−O(3a)	84.2(2)
O(4)−Ba−O(5a)	130.5(2)	O(6)−Ba−O(5a)	142.9(2)
N−Ba−O(5a)	67.2(2)	Ba−O(5)−C(7)	91.4(5)
Ba−O(6)−C(9)	167.1(9)		

Compound **5** crystallizes from pyridine as a mononuclear species with two types of trifluoroacetate ligands, a chelating ligand with a Ba−O_{acet} bond distance of 2.877(6) Å and a dangling ligand with a Ba−O_{acet} bond distance of 2.631(9) Å (Figure 5). The longer Ba−O_{acet} bond distances for chelating trifluoroacetate ligands, compared to dangling or bridging trifluoroacetate ligands, probably arises from the need to reduce ring strain in the Ba−O−C−O four-membered ring. Additional bond distances and angles for **5** are listed in Table 7. In **5**, the barium atom resides slightly out of the plane of the six oxygen atoms of the 18-crown-6 ether (*trans*-O_{ether}−Ba−O_{ether} angles of 152.3(2) and 157.9(1)°) toward the chelating trifluoroacetate ligand. The average Ba−O_{ether} bond distance is 2.847[18] Å. A pyridine ligand, bonded on the same side of the molecule as the chelating trifluoroacetate ligand, fills out the coordination sphere around the barium atom. The Ba−N bond distance of 2.934(8) Å is similar to that of **4**. Apparently, a Ba−pyridine interaction with dangling and chelating trifluoroacetate ligands is more favorable than having both trifluoroacetate ligands in a chelating mode with no pyridine. The coordination number in either case would be 10. The only other structurally characterized barium carboxylate compounds with 18-crown-6 ethers,

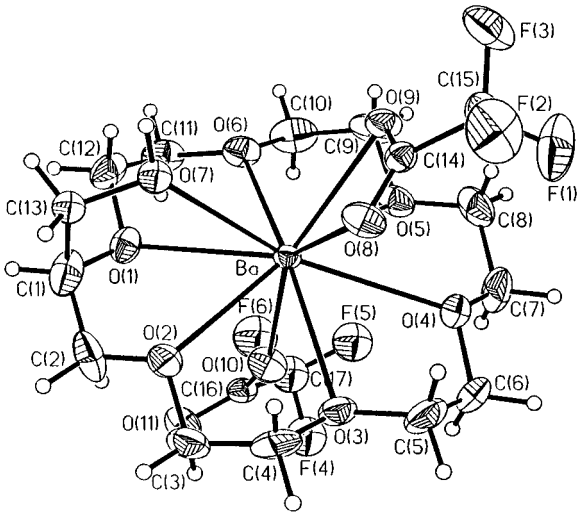

Figure 6. Molecular structure of $Ba(O_2CCF_3)_2$(18-crown-6CH_2OH) (**6**). Only one orientation of disordered atoms is shown. Thermal ellipsoids are scaled to the 20% probability level except for hydrogen atoms which have been given arbitrary thermal parameters for clarity.

$Ba(O_2C(CH_3)_3)_2$(18-crown-6),[32,38] $Ba(O_2CCH_3)_2$(18-crown-6)·$4H_2O$, and $Ba_2(O_2C(CH_2)_2CO_2)$(18-crown-6)·$6H_2O]_\infty$[31] are also 10 coordinate, but this coordination number is achieved by chelation of the carboxylate groups to the metal centers.

Compound **6** is mononuclear in the solid state and similar in structure to **5** with chelating and dangling trifluoroacetate groups and an 18-crown-6 ligand, bonded to the metal center through all six ether oxygen atoms, occupying a total of nine coordination sites (Figure 6). In both compounds the metal coordination number is 10, which seems to be the upper bound for these type of species, the tenth coordination site in **6** is filled by a hydroxyl group rather than a pyridine molecule as was the case for **5**. A selected listing of bond distances and angles for **6** is provided in Table 8. The Ba−O(7) hydroxy bond distance of 2.856(7) Å in **6** is not significantly different from that of **3**. As one might also expect, the $Ba-O_{acet}$ bond distances are similar to those of **5**. However, the $Ba-O_{ether}$ bond distances show a greater spread in their values (2.780(5)−2.862(5) Å) which may be attributable to effects of the coordinated hydroxymethylene group of the crown ether as was discussed for **3**. The monomeric $Ba(O_2CCF_3)_2$(18-crown-6CH_2OH) units in the crystal are joined together by intermolecular hydrogen bonds between the nonbonded oxygen atoms (O(11)) of the dangling trifluoroacetate ligands and protons of the hydroxymethylene groups.

Comparison of the structural data of the eight polydentate ligand adducts of barium trifluoroacetate (Table 2) provides the following ranges for the $Ba-O_{ether}$, $Ba-O_{acet}$ (bridging, chelating, and dangling), $C-O_{acet}$, and $O_{acet}-C-O_{acet}$ bond distances and angles: $Ba-O_{ether}$, 3.080(5)−2.762(6) Å (35 observations), $Ba-O_{acet}$, 2.790(6)−2.635(14) Å (bridging, 10 observations), 2.877(6)−2.773(4) Å (chelating, 4 observations), 2.813(10)−2.631(9) Å (dangling, 4 observations), $C-O_{acet}$, 1.25(1)−1.17(2) Å (26 observations), $O_{acet}-C-O_{acet}$, 132.0(8)−127.5(7)° (14 observations). The $Ba-O_{ether}$ bond distances cover a range of 0.3 Å. The two extremes correspond to special cases where the ether atom either *bridges* metal atoms ($[Ba_2(O_2CCF_3)_4$(tetraglyme)$]_\infty$)[28] or is in close proximity to a hydroxymethylene group involved in hydrogen bonding (**3**). The strong dependence of the $Ba-O_{acet}$ bond distances of the bridging, chelating, and dangling trifluoroacetate ligands on their chemical environments results in overlap of their ranges. However, in most cases the $Ba-O_{chelating}$ bond distances are longer than the $Ba-O_{dangling}$ or $Ba-O_{bridging}$ bond distances. The $C-O_{acet}$ bond distances cover a narrow range of 0.08 Å. Their relatively high esd's preclude any definitive statements on the significance of the differences; however, the purely dangling trifluoroacetate ligands of compounds **4** and **5** have long and short C−O bond distances of 1.221(8) and 1.194(9) Å and 1.213(14) and 1.195(13) Å, respectively. These values are all consistent with the presence of a C═O double bond. The $O_{acet}-C-O_{acet}$ angles span a range of 4.8°. The $O_{acet}-C-O_{acet}$ angles of bridging and dangling trifluoroacetate ligands are generally more obtuse than those of chelating ligands. This not unexpected since the O−C−O group in chelating ligands comprise three vertexes of the four-membered Ba−O−C−O ring.

Table 8. Selected Listing of Bond Distances (Å) and Angles (deg) for **6**[a]

Bond Distances			
Ba−O(1)	2.825(4)	Ba−O(2)	2.780(5)
Ba−O(3)	2.836(5)	Ba−O(4)	2.862(5)
Ba−O(5)	2.849(6)	Ba−O(6)	2.817(5)
Ba−O(7)	2.856(7)	Ba−O(7′)	2.863(14)
Ba−O(8)	2.845(5)	Ba−O(9)	2.827(5)
Ba−O(10)	2.677(6)		
Bond Angles			
O(1)−Ba−O(4)	157.3(2)	O(2)−Ba−O(5)	159.4(2)
O(3)−Ba−O(6)	160.5(l)	O(1)−Ba−O(7)	57.2(2)
O(2)−Ba−O(7)	63.2(2)	O(3)−Ba−O(7)	110.2(2)
O(4)−Ba−O(7)	144.9(2)	O(5)−Ba−O(7)	132.6(2)
O(6)−Ba−O(7)	83.5(2)	O(l)−Ba−O(8)	129.4(l)
O(2)−Ba−O(8)	91.2(2)	O(3)−Ba−O(8)	71.7(l)
O(4)−Ba−O(8)	72.O(2)	O(5)−Ba−O(8)	105.6(2)
O(6)−Ba−O(8)	126.9(2)	O(7)−Ba−O(8)	72.9(2)
O(1)−Ba−O(9)	124.5(2)	O(2)−Ba−O(9)	131.4(l)
O(3)−Ba−O(9)	110.6(l)	O(4)−Ba−O(9)	74.7(2)
O(5)−Ba−O(9)	68.9(2)	O(6)−Ba−O(9)	84.7(l)
O(7)−Ba−O(9)	80.6(2)	O(8)−Ba−O(9)	45.5(l)
O(1)−Ba−O(10)	73.5(2)	O(2)−Ba−O(10)	77.2(2)
O(3)−Ba−O(10)	73.6(2)	O(4)−Ba−O(10)	84.0(2)
O(5)−Ba−O(10)	82.3(2)	O(6)−Ba−O(10)	87.1(2)
O(7)−Ba−O(10)	126.9(2)	O(8)−Ba−O(10)	144.6(2)
O(9)−Ba−O(10)	150.1(2)	Ba−O(7)−C(13)	117.1(7)
Ba−O(8)−C(14)	92.1(4)	Ba−O(9)−C(14)	92.6(4)
Ba−O(10)−C(16)	157.2(6)		

[a] Primed atoms represent alternate positions for unprimed atoms.

NMR Spectroscopy. The ^1H NMR spectra of compounds **1**−**7** contain singlet, triplet, and multiplet peaks for the methylene linkages of the polydentate ligands and in the case of **5** and **6** additional peaks for coordinated pyridine and a hydroxymethylene group, respectively. The ^1H NMR peaks for the polydentate ligands of **1**−**7** have chemical shifts 0.1−0.2 ppm downfield (see Experimental Section) from the free ligand peaks in the same deuterated solvent. This suggests that the polydentate ligands remain associated with the barium centers even in coordinating solvents such as methanol and acetonitrile. The hydroxy proton of **3** in deuterated methanol was not observed probably due to exchange with the solvent. The chemical shifts of the methyl and methylene groups of **1**−**3** and **5**−**7** are in the range 3.4−3.8 ppm. Whereas the 12-crown-4 and 18-crown-6 polyether compounds have only one singlet peak in their spectra. The spectra of complexes with more unsymmetrical polyethers contain overlapping multiplets for the methylene groups. The ^1H NMR spectrum of compound **4** is well resolved with triplets at 2.71 and 3.74 ppm and a singlet at 3.66 ppm. The downfield triplet and singlet are reversed in

(38) Burns, J. H.; Bryan, S. A. *Acta Crystallogr., Sect. C: Cryst. Struct. Commun.* **1988**, *C44*, 1742.
(39) Timmer, K.; Meinema, H. A. *Inorg. Chim. Acta* **1991**, *187*, 99−106.

order for the uncoordinated cryptand. The triplet peaks can be assigned to the ethylene chains of the cryptand which are bonded through their ends to nitrogen atoms (2.71 ppm) and oxygen atoms (3.74 ppm). The $^2J_{H-H}$ coupling constant of 4.8 Hz is significantly smaller than the free ligand value of 5.7 Hz presumably due to a conformational change on coordination. The singlet peak arises from the six equivalent methylene groups of the three ethylene bridges along the waist of the kryptand.

The ^{13}C NMR spectra of **1**−**6** contain peaks in the upfield region 50−80 ppm corresponding to the carbon atoms of the polydentate ligands. The downfield region of each spectrum contains two quartets corresponding to the carbon atoms of the trifluoromethyl and carbonyl groups. The quartets arise from $^1J_{C-F}$ and $^2J_{C-F}$ coupling, respectively. The chemical shift and coupling constant ranges for the $-CF_3$ groups of **1**−**6** are 118.2−118.7 ppm and 293−299 Hz, respectively. The chemical shift and coupling constant ranges for the C(O) groups are 159.8−163.4 ppm and 31.7−34.7 Hz. The ranges are quite narrow for the carbon atoms of both functional groups suggesting that both the magnetic and chemical environments of the trifluoroacetate ligands in these compounds are similar. For comparison, the chemical shift (coupling constants) of the carbon atoms of the $-CF_3$ and C(O) groups of trifluoroacetic acid and $Ba(O_2CCF_3)_2$·THF are 115.0 ppm (284 Hz) and 163.0 ppm (43.7 Hz) and 118.2 ppm (291 Hz) and 163.5 ppm (35.3 Hz), respectively.

The ^{13}C NMR spectrum of compound **5**, in addition to the ether and trifluoroacetate peaks, contains singlet peaks in the range 125−150 ppm for the coordinated pyridine ligand. Compound **7** has a downfield quartet at 121.7 ppm (J_{C-F} = 319 Hz) for the $-CF_3$ group of the trifluoromethanesulfonate ligand.

IR Spectroscopy. The IR spectrum of each compound has characteristic peaks for the C−O−C stretching vibrations of the polydentate ligand in the range 1050−1250 cm^{-1}. Some of these peaks are shifted (ca. <10 cm^{-1}) to lower value compared to the same peaks for the free ligands, which is indicative of polydentate ligand coordination. For compounds **3** and **6**, broad O−H stretching vibrations are observed at 3316 and 3382 cm^{-1}, respectively. The free ligand O−H stretching vibrations occur at 3386 cm^{-1} for 15-crown-5CH_2OH and 18-crown-6CH_2OH. The differences between these frequencies can be attributed to both coordination of the hydroxyl groups of 15-crown-5CH_2OH and 18-crown-6CH_2OH to the metal center in **3** and **6** and changes in the hydrogen-bonding interactions of the coordinated ligands as compared to the free ligands.

A listing of frequencies for the $\nu_{asym}(CO_2)$ stretching vibration for **1**−**6** as well as other polydentate ligand adducts of group 2 metal carboxylates is given in Table 2. The $\nu_{sym}(CO_2)$ stretching vibrations for **1**−**3**, **5**, and **6** are much weaker than the asymmetric vibrations, and they could not be unambiguously assigned due to overlap with methylene bending vibrations of the polydentate ligands between 1430 and 1490 cm^{-1}. However, the $\nu_{sym}(CO_2)$ vibration in the spectrum of compound **4** could be assigned to a peak at 1406 cm^{-1} by comparison to the IR spectrum of the free cryptand(222). In a comparison of the $\nu_{asym}(CO_2)$ vibrations of **1**−**6** with those of nonhalogenated carboxylate compounds, it is evident that the trifluoromethyl groups of the trifluoroacetate ligands of **1**−**6**, through a strong electron-withdrawing effect, significantly increase the frequencies of the $\nu_{asym}(CO_2)$ vibrations. The $\nu_{asym}(CO_2)$ vibrations for **1**−**6**, $Ba_2(O_2CCF_3)_4$(15-crown-5)$_2$, and $[Ba_2(O_2CCF_3)_4$(tetraglyme)$]_\infty$, when examined in conjunction with their solid-state structures, provide qualitative information on the frequency region for bridging, chelating, and dangling trifluoroacetate ligands in this chemical environment. The bridging trifluoroacetate ligands of **1**, **2**, and $Ba_2(O_2CCF_3)_4$(15-crown-5)$_2$ give rise to high-frequency vibrations in the range of 1690−1717 cm^{-1}. With these assignments, one can then assign bridging trifluoroacetate ligands in compounds where this bonding mode and another are present. The $\nu_{asym}(CO_2)$ vibrations at 1704 cm^{-1} for **3** and 1689 cm^{-1} for $[Ba_2(O_2CCF_3)_4$(tetraglyme)$]_\infty$ should correspond to the bridging trifluoroacetate ligands of these compounds. The frequency of the dangling ligands of **4**, when taken with the frequencies of the dangling and chelating ligands of **5**, **6,** and $[Ba_2(O_2CCF_3)_4$(tetraglyme)$]_\infty$ provide a working range of 1654−1678 cm^{-1} for chelating and 1694−1700 cm^{-1} for dangling trifluoroacetate ligands. The chelating range does not overlap with the bridging and dangling ranges, at least for this group of compounds. However, the bridging and dangling ranges do overlap and a distinction between these two bonding modes in $Ba(O_2CCF_3)_2L$ compounds using only $\nu_{asym}(CO_2)$ vibrations is not possible. For compound **4**, where $\nu_{sym}(CO_2)$ could be assigned, the difference between $\nu_{asym}(CO_2)$ and $\nu_{sym}(CO_2)$ (i.e. Δ) is 288 cm^{-1}, which places the trifluoroacetate ligands of this compound in the Δ range developed by Deacon et al.[34] for dangling trifluoroacetate ligands. The above analysis, although based on the structures and IR data of only 8 compounds, provides the useful relationship $\nu_{asym}(CO_2$-chelating) < $\nu_{asym}(CO_2$-bridging) or $\nu_{asym}(CO_2$-dangling) for $Ba(O_2CCF_3)_2L$ compounds.

Throughout the above analysis no direct consideration was paid to the effect that the type of polydentate ligand or the number of coordinating atoms of this ligand have on the $\nu_{asym}(CO_2)$. The data in Table 2 suggest that $\nu_{asym}(CO_2)$ is primarily affected by the number of donating atoms of the polydentate ligand. For example, compounds **1** and **2** possess cyclic and acyclic, respectively, polyethers containing the same number of donating atoms (i.e. 4) and their $\nu_{asym}(CO_2)$ frequencies differ by only 3 cm^{-1}, whereas $Ba_2(O_2CCF_3)_4$(15-crown-5)$_2$ with a similar polyether but one more donating atom has a $\nu_{asym}(CO_2)$ ca. 30 cm^{-1} higher than **1** or **2**. A similar comparison may be made between **5** and **6**. The differences in these two compounds is primarily in the coordination of pyridine for **5** and a hydroxyl group for **6**. The chelating trifluoroacetate ligand of **5** has a $\nu_{asym}(CO_2)$ frequency 9 cm^{-1} higher than that of **6**. The increase in $\nu_{asym}(CO_2)$ frequency in this case is probably a consequence of the better donating ability of pyridine resulting in a greater increase in the C−O bond order of the chelating trifluoroacetate ligand of **5** over that of **6**. In general, the $\nu_{asym}(CO_2)$ vibrations of the $[Ba(O_2CCF_3)_2]_mL_n$ (m = n) compounds in Table 2 are 10−55 cm^{-1} higher than that of $Ba(O_2CCF_3)_2$·THF (Table 2). Clearly, this suggests that the barium−polydentate ligand interaction is significant and results in an increase in the C−O bond order of the trifluoroacetate ligands of $[Ba(O_2CCF_3)_2]_mL_n$ compounds. For comparative purposes, the $\nu_{asym}(CO_2)$ of neat CF_3COOH is 1782 cm^{-1}.

Thermogravimetric Analyses. Compounds **1**−**7** were examined by TGA in dry air to investigate their thermal decomposition behavior. It has been demonstrated previously that nonfluorinated group 2 carboxylate compounds decompose to the thermodynamically favorable metal carbonates when heated in air (Table 2). For compounds **1**−**5** and **7**, BaF_2 is the main product of thermal decomposition in air as determined by both powder X-ray diffraction and TGA mass loss. Similar decomposition behavior has also been found for the fluorinated β-diketonate polyether adducts of the group 2 metals. MF_2 would seem to represent a thermodynamic well for these

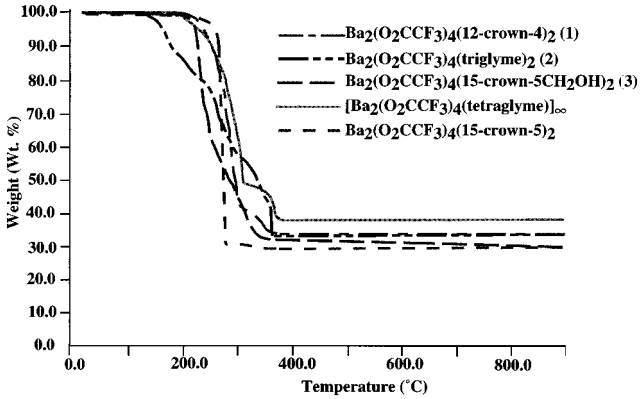

Figure 7. TGA graphs of weight loss (%) versus temperature (°C) for **1**−**3**, $Ba_2(O_2CCF_3)_4$(15-crown-5)$_2$, and $[Ba_2(O_2CCF_3)_4$(tetraglyme)$]_\infty$.

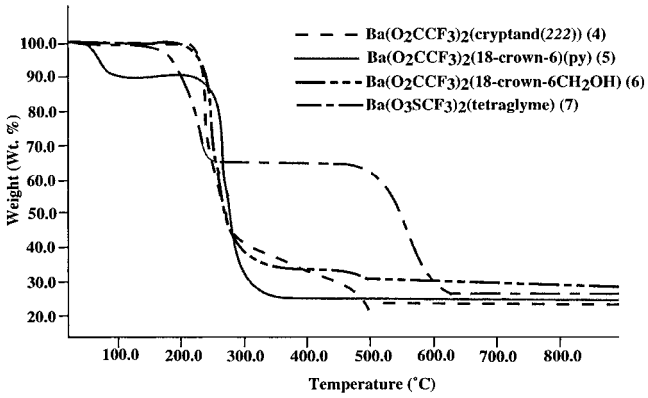

Figure 8. TGA graphs of weight loss (%) versus temperature (°C) for **4**−**7**.

fluorinated species. Particular features of the TGA graphs for **1**−**7** vary. Compounds **1** and the previously reported $Ba_2(O_2CCF_3)_4$(15-crown-5)$_2$[28] behave similarly decomposing over a narrow temperature range of 250−320 °C in one well-defined step. This is in contrast to the analogous nonfluorinated carboxylate compounds which undergo dissociation of the polyether ligand at ∼150 °C to form the corresponding metal carboxylate which thermally decomposes to form the metal carbonate at 400−600 °C.[31] The decomposition of compound **5** follows this pattern where the decomposition to BaF_2 between 250 and 300 °C is preceded by loss of coordinated pyridine at 100 °C. The TGA graphs of compounds **2**−**4** and **6** indicate that these compounds decompose over larger temperature ranges with no distinct or identifiable steps. An X-ray powder pattern of the TGA residue of compound **6** shows that both $BaCO_3$ and BaF_2 are formed, reproducibly, during its decomposition. This compound represents the only example of a fluorinated barium carboxylate that we have studied that does not exclusively go to BaF_2 during thermal decomposition. The reason for this behavior has not yet been determined. Compound **7**, the only non-carboxylate of the group decomposes in two well-defined steps; it losses tetraglyme at 190−255 °C to give, presumably, $[Ba(CF_3SO_3)_2]_n$, which then decomposes to BaF_2 between 500 and 620 °C. The same decomposition products and similar decomposition behavior for **1**−**7** are observed when the TGA experiments are conducted under dinitrogen. TGA plots of **1**−**3**, $Ba_2(O_2CCF_3)_4$(15-crown-5)$_2$, and $[Ba_2(O_2CCF_3)_4$(tetraglyme)$]_\infty$ and **4**−**7** are shown in Figures 7 and 8, respectively.

Conclusion

In this paper we have described the synthesis, structures, NMR spectra, thermal behavior, and IR data for a group of polydentate ligand adducts of barium trifluoroacetate. The compounds can be obtained in anhydrous form by a facile reaction between BaH_2, polydentate ligand, and trifluoroacetic acid in THF solvent. All compounds have good solubility in alcohols but do not sublime intact when heated under vacuum, making them unsuitable for CVD of Ba-containing films using conventional delivery methods. Compounds **1**−**6** have mononuclear and dinuclear structures in the solid state and are the first structurally characterized adducts of $Ba(O_2CCF_3)_2$. While nonfluorinated barium carboxylates thermally decompose to $BaCO_3$, these fluorinated compounds thermally decompose in air to BaF_2. By collation of the structural and IR data for $[Ba(O_2CCF_3)_2]_mL_n$ compounds, wavenumber ranges corresponding to the bonding modes of the trifluoroacetate ligands for this class of compounds were developed. We hope to be able to use these ranges to aid identification of intermediates in the thermal reactions of these compounds.

Acknowledgment. We thank Texas Instruments for financial support of this work, the NSF chemical instrumentation program for the purchase of a low-field NMR spectrometer, and AFOSR and the Camille and Henry Dreyfus Foundation for the purchase of an X-ray diffractometer.

Supporting Information Available: X-ray crystallographic files, in CIF format, for complexes **1**−**6** are available on the Internet only. Access information is given on any current masthead page.

IC9613220